

# Rapid Free Surface Simulation for Steady-State Hull Resistance with FVM using OpenFOAM

Hrvoje Jasak<sup>1,2</sup>, Vuko Vukčević<sup>1</sup> and Dominik Christ<sup>2</sup>  
(<sup>1</sup>Faculty of Mechanical Engineering and Naval Architecture,  
Zagreb/Croatia, <sup>2</sup>Wikki Ltd., UK)

## ABSTRACT

This work describes a novel method to calculate resistance force at steady forward motion with free-surface simulation using the viscous turbulent flow model in Volume-Of-Fluid (VOF) formulation. Assuming quasi steady-state solution, equations for fluid flow and free-surface motion are decoupled due to separation of time-scales. It is thus possible to increase the time-step size by about 3 orders of magnitude and preserve numerical stability, which gives a substantial increase in computational efficiency. The method has been implemented and tested in foam-extend, a fork of the OpenFOAM software.

KCS and DTMB hull geometries are simulated with the novel method and results are compared with experimental data. The accuracy is equal to simulations with a conventional transient approach. Performance and parallel scalability are assessed. The results show that the novel method delivers substantially increased computational efficiency without sacrifice of accuracy.

## INTRODUCTION

Calculation of the resistance force of ship hulls at steady forward motion is one of the main applications of CFD in naval hydrodynamics. Resistance calculation is commonly carried out for a large number of design variants, often within an optimization loop. As a consequence, efficient use of available numerical resources is crucial. For this reason, potential flow and inviscid Boundary Element Method (BEM) simulations are still popular in industrial application (see Bertram, 2012) although they neglect substantial features of the flow. The Finite Volume Method (FVM) includes these features; however, it requires dividing the computational volume into small cells and the number of cells determines both computational cost and achievable accuracy (see e.g. Rhee and Skinner,

2006). Various publications (e.g. Enger et al., 2010) show the feasibility of calculating resistance force with available FVM codes. The motivation of this work is to increase the efficiency of calculating the resistance force with FVM by an order of magnitude. A novel approach based on separation of time-scales of the flow variables is described. Validation and performance results are presented for simulation of KCS and DTMB hulls. The simulations show that a substantial performance increase can be realized.

## APPROACH

The approach presented in this work captures the free-surface location with a VOF approach. The governing equations are:

- Volumetric continuity equation:

$$\nabla \cdot \mathbf{u} = 0, \quad (1)$$

where  $\mathbf{u}$  is the velocity field reformulated in terms of pressure. To ensure smooth numerics, buoyancy is removed from the momentum equation and built into the pressure. Decomposition reads

$$p = p_d + \rho gh, \quad (2)$$

where  $p$  stands for static pressure and  $\rho gh$  is its hydrostatic component. The pressure equation is formulated in terms of  $p_d$ .

- Combined momentum equation for the two-phase system, assuming phase separation:

$$\frac{\partial(\rho \mathbf{u})}{\partial t} + \nabla \cdot (\rho \mathbf{u} \mathbf{u}) - \nabla \cdot \boldsymbol{\sigma} = -\nabla p + \rho \mathbf{g} \quad (3)$$

- Phase continuity equation defined in terms of volume fraction variable  $\alpha$ , derived from phase mass conservation:

$$\frac{\partial \alpha}{\partial t} + \nabla \cdot (\mathbf{u} \alpha) = 0 \quad (4)$$

- Density  $\rho$  and viscosity  $\nu$  are calculated explicitly from their single phase values:

$$\rho = \alpha\rho_1 + (1 - \alpha)\rho_2, \quad (5)$$

$$\nu = \alpha\nu_1 + (1 - \alpha)\nu_2, \quad (6)$$

accounting for the location of the free surface.

The phase continuity equation (Eq. 4) is hyperbolic and its numerical stability is governed by the Courant-Friedrichs-Lewy(CFL)-number:

$$CFL = \frac{u\Delta t}{\Delta x} \leq CFL_{\max} \quad (7)$$

The divergence term of the phase continuity equation is zero in all cells away from the free-surface because in the gas phase,  $\alpha = 0$  and thus  $\nabla \cdot (\mathbf{u}\alpha) = 0$ , or  $\alpha = 1$  in the liquid phase with continuity equation giving  $\nabla \cdot \mathbf{u} = 0$ . This allows us to define a special free-surface CFL-number  $CFL_{FS}$  that includes only the part of  $CFL$  in cells with  $0 < \alpha < 1$ . This shows that two separate time-scales are relevant in the set of governing equations, the time-scale of the fluid flow and the time-scale of the free-surface motion. This is most obvious as steady-state is approached, where the free-surface does not move at all, while the fluid is flowing at the speed of steady forward motion.

Accurate calculation of the resistance force requires a well resolved boundary layer, which leads to small cell size normal to the hull surface. These length scales affect the fluid CFL-number in areas, where mesh and fluid flow are not perfectly aligned, especially around inflow and outflow. The motion of the free-surface, which is perpendicular to the hull, is unaffected by this. Therefore, we can run the simulation at  $CFL_{\max} \approx 1000$  for the fluid flow and  $CFL_{FS, \max} \approx 1$  for the free-surface motion. Under such conditions, the fluid flow is in quasi steady-state:  $\frac{\partial \rho \mathbf{u}}{\partial t} = 0$  can be assumed. This assumption decouples fluid flow and free-surface motion and increases possible free-surface displacement in a each time-step. In practice, we solve fluid flow equations using segregated iterative methods and the loss of the  $\frac{\partial \rho \mathbf{u}}{\partial t}$  term can be interpreted as the fluid flow solution relaxing towards the current shape of the free-surface.

The VOF approach usually applies interface sharpening measures that counteract the numerical diffusion of the volume fraction variable. Commonly, numerical discretization schemes with negative numerical diffusivity are applied, see Ubbink (1997). The schemes act on the convection term of the phase continuity equation and their effect thus depends on the amount of free-surface motion. A stationary free-surface is not sharpened at

all, while a large displacement leads to an exaggerated sharpening which damages numerical stability. The presented approach thus applies the method from Rusche (2002) that introduces an additional term into the transport equation with relative velocity  $\mathbf{u}_r$  oriented toward and normal to the free-surface:

$$\frac{\partial \alpha}{\partial t} + \nabla \cdot (\mathbf{u}\alpha) + \nabla \cdot [\mathbf{u}_r \alpha (1 - \alpha)] = 0, \quad (8)$$

where  $\mathbf{u}_r$  is calculated from numerical considerations.

A typical issue of the VOF approach is the occurrence of parasitic velocities in the gas phase. These occur in partially filled cells ( $0 < \alpha < 1$ ) with outgoing flux through faces that are submerged in the liquid to a degree larger than  $\alpha$ . The outgoing momentum is weighted by the value of  $\alpha$  in the cell and thus the outgoing momentum flux is under-predicted. Due to the high density ratio between water and air, comparably small differences in liquid phase momentum cause high velocities in the gas phase. In the approach presented here, this effect is countered quite pragmatically by explicitly clipping all velocities above a  $U_{\text{limit}}$  value. The value for  $U_{\text{limit}}$  must be chosen to be sufficiently large not to interfere with the flow in the liquid phase, but sufficiently small to contain the parasitic velocities effectively.

The novel approach has been implemented into the open source FVM software library foam-extend (a forked version of the OpenFOAM software), Weller et al. (1998). Various aspects have been validated on geometries of the MOERI container ship (KCS) and the DTMB 5415 US Navy combatant. These include:

- Total and residuary resistance coefficients (KCS and DTMB)
- Wave profiles (KCS and DTMB)
- Mesh refinement dependency (KCS)
- Influence of  $U_{\text{limit}}$  parameter (KCS)
- Comparison with transient simulation (KCS)
- Parallel scalability (DTMB)

### MOERI container ship (KCS)

Accuracy and performance of the novel quasi-steady approach are assessed by simulating the steady resistance of the MOERI container ship (KCS) at model scale ( $L_{pp} = 7.2786$ ). A

half model was simulated with symmetry conditions. Boundary conditions and fluid properties were set up to provide  $Re=1.4 \times 10^7$  and  $Fr=0.26$ . The boundaries on bottom, top and farfield side of the domain were specified as slip walls. The convective term was discretized with a second order upwind scheme for momentum and a TVD-scheme with **van Leer** limiter for the volume fraction variable  $\alpha$ . The time-derivative term in the  $\alpha$  transport equation (Eq. 4) was discretized with a first order implicit Euler scheme. This is sufficient, since time-accuracy is not relevant for reaching a steady-state.

Simulations were run with three different meshes with sizes between 1.13M cells and 4.06M cells to determine the influence of mesh refinement. Mesh parameters and resistance coefficients are given in Table 1.

Table 1: Mesh refinement results for steady resistance of KCS hull

mesh no.	1	2	3
cells	1.13M	2.04M	4.06M
average $y^+$	66	32	32
$CFL_{max}$	342	871	1012
$c_t$	$3.570 \times 10^{-3}$	$3.599 \times 10^{-3}$	$3.489 \times 10^{-3}$
diff. EFD	0.38%	1.18%	-1.91%
$c_r$	$0.758 \times 10^{-3}$	$0.787 \times 10^{-3}$	$0.677 \times 10^{-3}$
diff. EFD	4.61%	8.56%	-6.59%

The CFD results for total resistance coefficient  $c_t$  are within  $\pm 2\%$  of the experimental value from Kim et al. (2001), where the experimental uncertainty is given as  $\pm 1\%$ . The accuracy achieved by the quasi-steady approach is similar to other CFD studies of KCS steady resistance, which have been undertaken with different CFD software and a transient approach (e.g. Enger et al., 2010; Zhang, 2010; Seo et al., 2010). The values of  $c_t$  and  $c_r$  do not follow a trend with increasing mesh refinement. According to ITTC (2002), the mesh convergence should be thus classified as oscillatory, although within a narrow range.

Figure 1 shows the evolution of resistance coefficients  $c_r$ ,  $c_f$  and  $c_t$  as iterations proceed. The values stabilize after about 2500 iterations. It is notable that the residual resistance coefficient  $c_r$  oscillates around its final value, while the frictional resistance coefficient  $c_f$  is stable. This oscillation is caused by motion of the free surface, which periodically attaches and detaches from the stern. This behavior has been observed experimentally as well. The transom stern is designed to stay dry above the water surface. However, at operating speed,

waves rise “over the transom stern and flow reversal behind the transom” (Kim et al., 2001). In the simulation, this causes pressure fluctuations on the stern surface that become oscillations in the residual resistance coefficient.

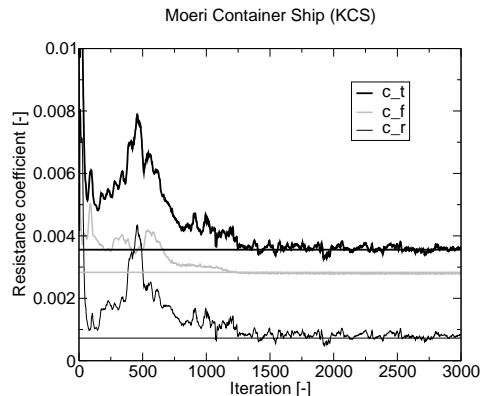


Figure 1: Convergence of resistance coefficients  $c_t$ ,  $c_f$  and  $c_r$  for KCS hull with number of iterations. Steady value  $c_t = 3.559 \times 10^{-3}$  is reached after about 2500 iterations.

The wave pattern generated by the KCS hull is shown in Figure 2 and compared to experimental data from Kim et al. (2001). The wave profiles at positions  $y/L=0.082$  and  $y/L=0.1509$  show good agreement with experimental results until about  $x/L=1.3$  and  $x/L=1.6$ , respectively. Further downstream, the wave amplitude is under-predicted and the wave peaks are slightly shifted forward. Away from the hull, at  $y/L=0.4224$ , the simulation over-predicts the amplitudes of the first three waves, but matches the experimental results closely further downstream. The overall wave pattern of EFD and CFD are similar in their features as well.

The influence of parameter  $U_{limit}$  was investigated separately because it potentially interferes with the flow fields on a fundamental level. This parameter limits the maximum velocity in the domain in order to mitigate parasitic velocities in the gas phase. The value of  $U_{limit}$  must be therefore sufficiently large compared to the highest velocity in the liquid phase. In the simulations shown above,  $U_{limit}$  was set to 20 m/s, which is about one order of magnitude larger than the inlet velocity of  $U_{inlet} = 2.1964$  m/s. Larger values do not reduce parasitic velocities in the gas phase effectively enough and thus impact solution stability. Smaller values for  $U_{limit}$  were tested using 5 m/s, 10 m/s, and 15 m/s. Figure 3 shows the resulting total re-

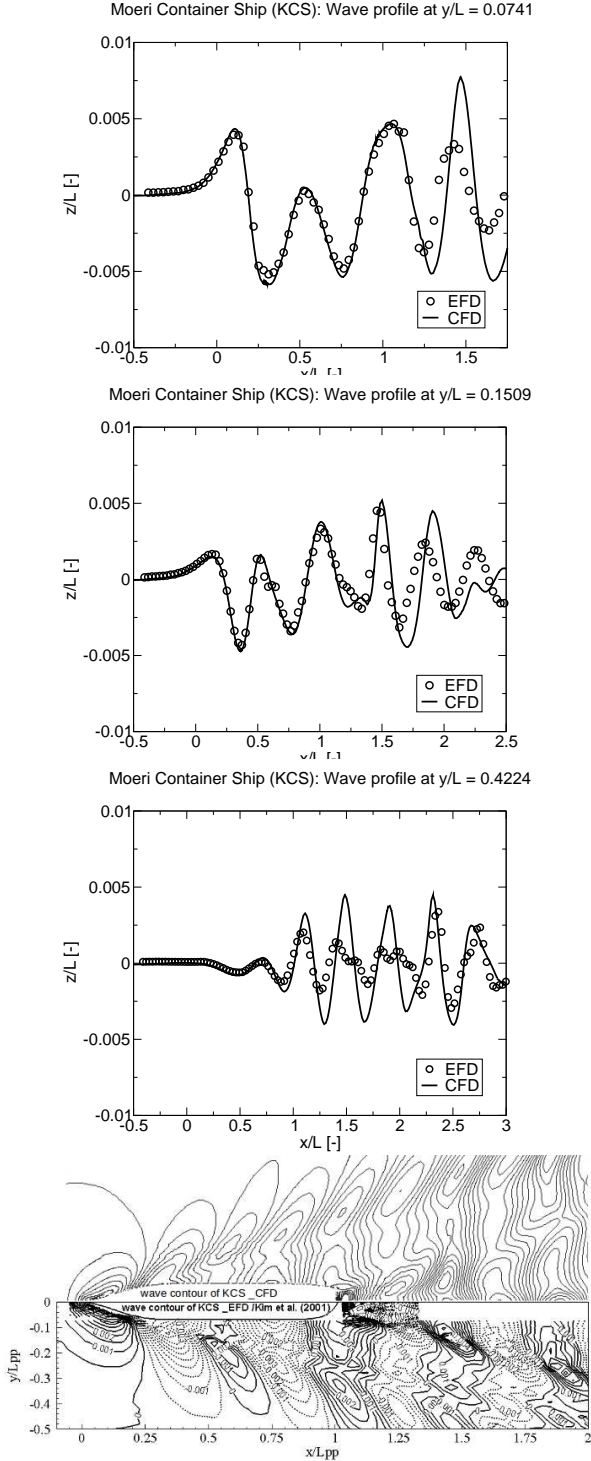


Figure 2: Wave profiles and overall wave pattern for KCS hull. The data of the finest mesh are shown.

istance coefficient  $c_t$ , which is almost unaffected with only a very slight decrease as  $U_{\text{limit}}$  is lowered. The solution is therefore not sensitive to the chosen value of  $U_{\text{limit}}$ , even for values as low as

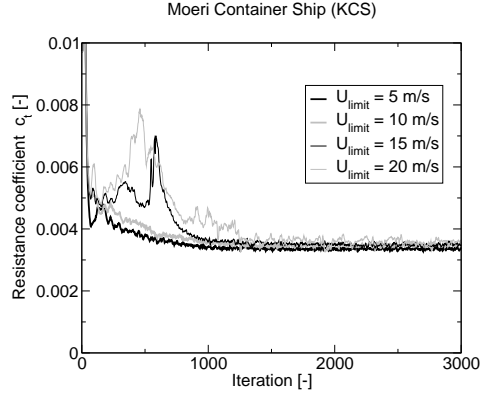


Figure 3: Influence of parameter  $U_{\text{limit}}$  on total resistance coefficient

about  $2 \times U_{\text{inlet}}$ .

The motivation for the quasi-steady approach is to achieve a significant speed-up and reduction of computational cost for steady resistance simulations. To evaluate the difference, steady resistance of the KCS hull was simulated on the coarsest mesh with a conventional transient approach. The transient simulation was set up to achieve quick convergence with a time-step corresponding to  $CFL_{\text{max}} \approx 4$ . All transient terms were discretized with a first-order implicit Euler scheme as time accuracy is not critical for achieving steady-state conditions.

Figure 4 compares the convergence of transient and quasi-steady simulation. The quasi-steady approach requires less than half of the iterations of the transient approach to reach a steady value for resistance. Furthermore, the resistance value of the quasi-steady approach is much less affected by the unsteadiness of the free-surface interactions at the stern of the KCS hull. This results in much smaller oscillations.

The computational cost is further reduced as one iteration for the quasi-steady approach requires about 2.9 times less time than one iteration with the transient approach. Overall, time and computational cost are reduced in this case by a factor of 6.

### DTMB 5414 US Navy combatant

For additional validation, the quasi-steady approach has been validated with a second hull geometry, the DTMB 5414 US Navy combatant. Steady resistance was simulated at model scale ( $L_{\text{pp}} = 5.719$ ) with a 13M cell mesh. A half model was used with symmetry boundary conditions. Inlet boundary conditions and fluid properties were ad-

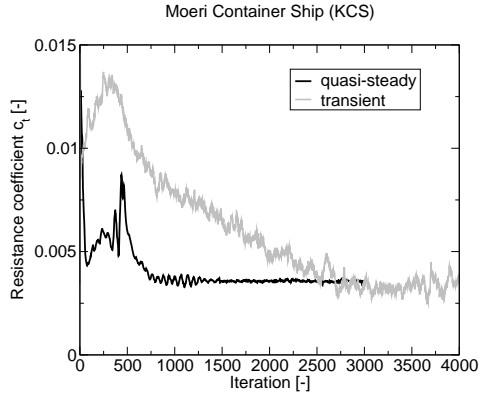


Figure 4: Comparison of convergence of the new quasi-steady approach and conventional transient simulation. Each transient iteration requires about 2.9 times more computational time compared to the quasi-steady approach.

justed for operating conditions at  $Re=1.19 \times 10^7$  and  $Fr=0.28$ . The  $U_{limit}$  parameter was set to 15 m/s. Otherwise, the numerical setup was identical to the simulation of KCS hull steady resistance. At steady-state, the simulation runs at  $CFL_{max} = 11300$ . At the hull surface, an average  $y^+ = 45$  is achieved.

The resistance coefficients in Figure 5 converge to a steady value after about 3000 iterations. As there are no transient interactions between free-surface and stern, as in the case of KCS hull, the residuary resistance coefficient  $c_r$  shows no oscillations. It converges to a value of  $1.31 \times 10^{-3}$ , which is a deviation of -0.8% from the experimental value from Olivieri et al. (2001). The total resistance coefficient is  $4.31 \times 10^{-3}$ , a difference of 1.95% from the experimental value. The achieved accuracy is similar to other FVM-CFD studies in literature that use a conventional transient approach (e.g. Jones and Clarke, 2010; Feng et al., 2010; Wood et al., 2007).

Figure 6 shows the wave profile generated by the DTMB hull. Overall, the location of all peaks is reproduced very accurately in the full range of  $-0.5 < x/L < 3$ . At  $y/L = 0.082$ , the CFD results for the first wave peak are slightly stretched forward, which results in a broader distribution and lower peak value. Furthermore, the trough at  $x/L = 1.3$  is under-predicted by the simulation. Otherwise, there is a good agreement between experimental and simulation results. Further away from the hull, at  $y/L = 0.172$  and  $y/L = 0.301$ , the second wave peak is slightly under-predicted, but otherwise experimental and

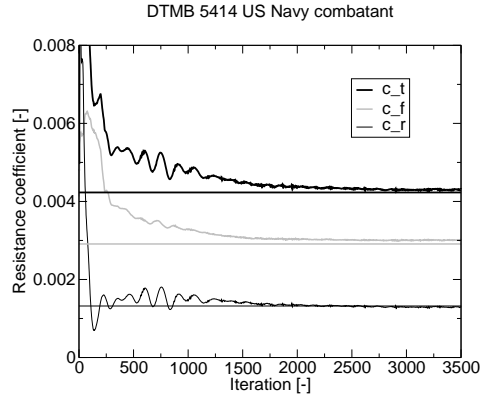


Figure 5: Convergence of resistance coefficients  $c_t$ ,  $c_f$  and  $c_r$  for DTMB hull with number of iterations. Steady value  $c_t = 4.31 \times 10^{-3}$  is reached after about 3000 iterations.

numerical results are very close. A comparison of the overall wave pattern shows similar structures and free surface elevation.

The DTMB case was also used to perform a scalability study, which shows the code performance in parallel computation. The same case setup was run on a cluster with 8, 16, 32 and 64 parallel processes. Results in Figure 7 show that simulations with the quasi-steady approach scale almost linearly. The lowest number of cells per process was about 200k for the 64 processor run.

## CONCLUSIONS

In this work, a novel approach is presented for the simulation of steady resistance with FVM-CFD. The approach uses a quasi steady-state approximation, which allows separation of time-scales for free-surface movement and fluid flow. This overcomes the CFL-number limit for the fluid flow and allows simulations at  $CFL_{max} \sim 1000$ . The necessary number of iterations to reach a steady value for resistance coefficients is about halved compared to conventional transient simulation. Furthermore, the computational cost for each iteration is much smaller. The total simulation time and computational cost is therefore significantly improved.

This work uses the KCS and DTMB hull geometries to validate the accuracy of the novel approach, which proves to be similar to conventional transient simulations. Furthermore, the performance improvement is quantified and shown to be about 6 times faster for the KCS hull simulation. Parallel performance is tested as well and the



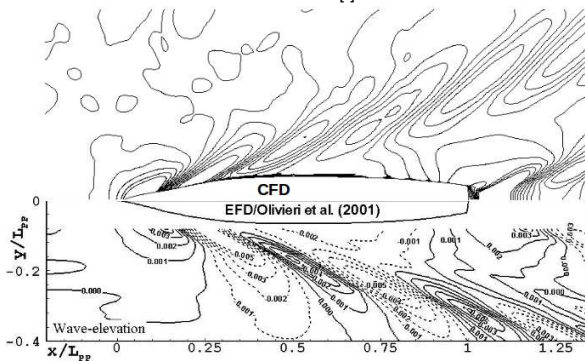
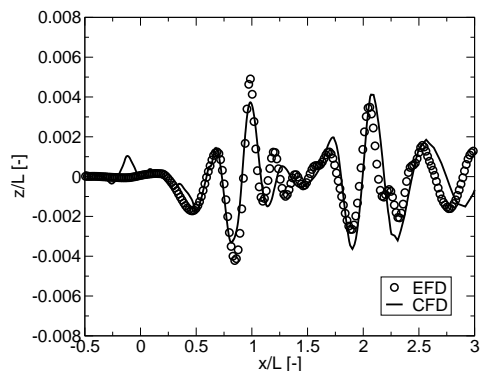
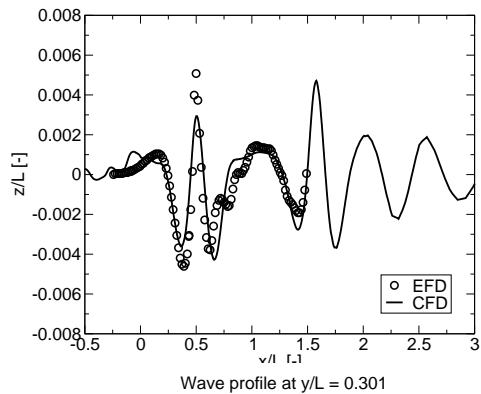
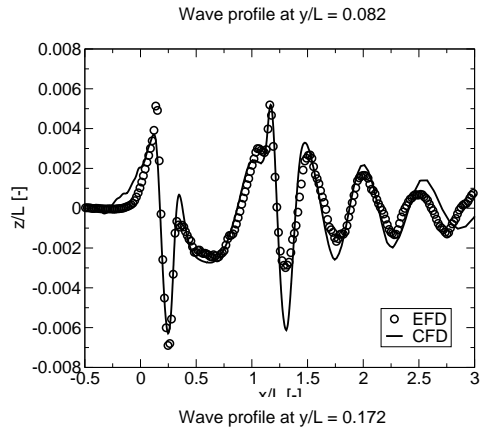


Figure 6: Wave profiles and overall wave pattern for DTMB hull.

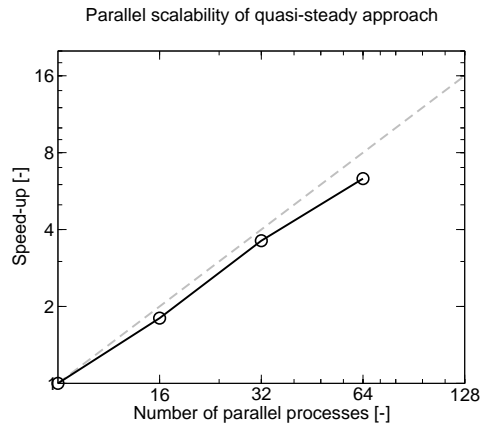


Figure 7: Scaling of the quasi-steady approach with increasing number of parallel processes

quasi-steady approach shows almost linear speed-up for runs with up to 64 processes.

## ACKNOWLEDGEMENT

The authors would like to thank Anders Östman from MARINTEK Ship Technology for providing meshes for the KCS hull simulations.

## REFERENCES

Bertram, V. *Practical Ship Hydrodynamics*. Elsevier Ltd., 2nd edition, 2012.

Enger, S., Perić, M., and Perić, R. Simulation of flow around KCS-hull. In Larsson, L., Stern, F., and Visonneau, M., editors, *Gothenburg 2010 - A Workshop on Numerical Ship Hydrodynamics, Proceedings, Volume II*, 2010.

Feng, X.-M., Chen, H.-M., Wu, Q., Yu, H., Wang, J.-B., and Cai, R.-Q. Prediction of 5415 resistance and wave pattern using multi-block structural grid. In Larsson, L., Stern, F., and Visonneau, M., editors, *Gothenburg 2010 - A Workshop on Numerical Ship Hydrodynamics, Proceedings, Volume II*, 2010.

ITTC. Recommended procedures and guidelines CFD, general uncertainty analysis in CFD verification and validation methodology and procedures. Technical report, International Towing Tank Conference, 2002.

Jones, D. and Clarke, D. Fluent code simulation of flow around a naval hull: the DTMB 5415. Technical Report DSTO-TR-2465, Australian Government Department of Defence, Defence Science and Technology Organisation, Maritime Platforms Division, 2010.

Kim, W. J., Van, S. H., and Kim, D. H. Measurement of flows around modern commercial ship models. *Experiments in Fluids*, 31, 2001.

Olivieri, A., Pistani, F., Avanzini, A., F. Stern, and Penna, R. Towing tank experiments of resistance, sinkage and trim, boundary layer, wake, and free surface flow around a naval combatant INSEAN 2340 model. Technical Report

IIHR Technical Report No. 421, Iowa Institute of Hydraulic Research, The University of Iowa, 2001.

Rhee, S. and Skinner, C. Computational validation of flow around surface ships using unstructured grid based RANS method. *International Journal of Maritime Engineering*, 148, Part A4:1–18, 2006.

Rusche, H. *Computational Fluid Dynamics of Dispersed Two-Phase Flows at High Phase Fractions*. PhD thesis, Imperial College of Science, Technology & Medicine, 2002.

Seo, J., Seol, D., Lee, J., and Rhee, S. Flexible CFD meshing strategy for prediction of ship resistance and propulsion performance. *International Journal of Naval Architecture and Ocean Engineering*, 2:139–145, 2010.

Ubbink, O. *Numerical Prediction of Two Fluid Systems with Sharp Interfaces*. PhD thesis, Imperial College of Science, Technology & Medicine, 1997.

Weller, H., Tabor, G., Jasak, H., and Fureby, C. A tensorial approach to computational continuum mechanics using object-oriented techniques. *Computers In Physics*, 12(6): 620–631, 1998.

Wood, M. P., González, L. M., Izquierdo, J., Sarasquete, A., and Rojas, L. P. RANSE with free surface computations around fixed DTMB 5415 model and other baliño's fishing vessels. In *9th International Conference on Numerical Ship Hydrodynamics Michigan, USA, 5-8 August, 2007*.

Zhang, Z. Verification and validation for RANS simulation of KCS container ship without/with propeller. In *9th international Conference on Hydrodynamics, October 11-15, 2010 Shanghai, China, 2010*.